

BCSJ Award Article

Isolable Iron(II)–Porphycene Derivative Stabilized by Introduction of Trifluoromethyl Groups on the Ligand Framework#

Kazuyuki Ito,[1] Takashi Matsuo,[1] Isao Aritome,[2] Yoshio Hisaeda,[2] and Takashi Hayashi*[1]

[1]Department of Applied Chemistry, Graduate School of Engineering, Osaka University, Suita, Osaka 565-0871

[2]Department of Chemistry and Biochemistry, Graduate School of Engineering, Kyushu University, Fukuoka 819-0395

Received July 9, 2007; E-mail: thayashi@chem.eng.osaka-u.ac.jp

Two iron porphycene complexes having four trifluoromethyl groups, chloro-2,7,12,17-tetraethyl-3,6,13,16-tetrakis-(trifluoromethyl)porphycenatoiron(III) [$Fe^{III}ClEtio(CF_3)_4Pc$] and its μ-oxo dimer [$\{Fe^{III}Etio(CF_3)_4Pc\}_2(\mu$-O)], were characterized. The μ-oxo dimer was easily converted into the monomeric iron(II) complex via the Fe–O bond cleavage in pyridine. This is the first study to obtain a stable iron(II) species in a series of porphycene iron complexes. The iron(II) species crystallized in the monoclinic system $C2/m$, and the Fe–$N_{pyridyl}$ (2.007 Å) and Fe–$N_{pyrrolyl}$ (1.958 Å) bonds were remarkably short distances among the bispyridine-coordinated iron(II) porphyrins and porphyrinoids. To evaluate the influences of the CF_3 substituents and framework structure on the autoreduction, we compared the reactivity of [$\{Fe^{III}Etio(CF_3)_4Pc\}_2(\mu$-O)] in pyridine with the reference iron porphycene and porphyrins. Autoreduction of [$\{Fe^{III}Etio(CF_3)_4Pc\}_2(\mu$-O)] smoothly proceeded at 20 °C in pyridine, whereas the reaction of the μ-oxo-bis{2,7,12,17-tetraethyl-3,6,13,16-tetramethylporphycenatoiron(III)} [$\{Fe^{III}Etio(CH_3)_4Pc\}_2(\mu$-O)] was converted into the monomeric iron(III) complex, and the iron(II) species was not available. In contrast, the μ-oxo-bis{1,3,5,7-tetrakis(trifluoromethyl)-2,4,6,8-tetraethylporphyrinatoiron(III)}[$\{Fe^{III}Etio(CF_3)_4Por\}_2(\mu$-O)] as a structural isomer of [$\{Fe^{III}Etio(CF_3)_4Pc\}_2(\mu$-O)] allowed the autoreduction, although the reaction was very slow and took over one month. These results indicate that the introduction of strong electron-withdrawing groups at the pyrrole β-carbons exhibits a unique reactivity of the iron complex.

It is of particular interest to compare the structure, physicochemical properties, and chemical reactivities of metalloporphycenes with those of metalloporphyrins, because the porphycene is a structural isomer of porphyrin with decrease in its framework symmetry from D_{4h} to D_{2h}.[1] According to the electrochemistry of porphyrin and porphycene, one of the important characteristics of the porphycene is that the LUMO energy level of its tetrapyrrole macrocycle is significantly lower than that of the porphyrin.[2–4] In contrast, it is well-known that the introduction of electron-withdrawing groups at the peripheral position of the porphyrin framework stabilizes its LUMO energy level of the macrocycle.[5–9] Thus, it seems interesting to introduce electron-withdrawing groups at the peripheral positions of the porphycene to obtain an electron-deficient macrocycle,[10–14] although almost all porphycenes have only simple alkyl side chains as peripheral substituents such as methyl, ethyl, or butyl groups on the framework.[15–17]

To further stabilize the LUMO energy level of porphycene, we have recently prepared the trifluoromethylated porphycene, 2,7,12,17-tetraethyl-3,6,13,16-tetrakis(trifluoromethyl)porphycene, $Etio(CF_3)_4PcH_2$.[10] The four electron-withdrawing trifluoromethyl substituents provided an attractive electron-deficient nature with a dramatically decreased HOMO–LUMO gap in the porphycene framework. In addition, we initially determined that its iron μ-oxo complex, [$\{Fe^{III}Etio(CF_3)_4Pc\}_2$-($\mu$-O)] (**1**), was readily converted into a monomeric iron(III) species, [$Fe^{III}Etio(CF_3)_4Pc(py)_2$] (**2-Py$_2$**), via the Fe–O bond cleavage and then reduced to a iron(II) complex in pyridine solution.[11,18] In this paper, we wish to utilize iron porphycenes without any electron-withdrawing groups, [$\{Fe^{III}Etio(CH_3)_4$-$Pc\}_2(\mu$-O)] (**3**) and [$Fe^{III}ClEtio(CH_3)_4Pc$] (**4-Cl**), and the corresponding iron porphyrins, [$Fe^{III}ClEtio(CF_3)_4Por$] (**5-Cl**) and [$\{Fe^{III}Etio(CF_3)_4Por\}_2(\mu$-O)] (**6**), to discuss the mechanisms of the unusual fast Fe–O bond cleavage and the following autoreduction of **1** (Chart 1).[18–20] Furthermore, we describe the first example of the crystal structure of the 6-coordinated iron(II) porphycene complex.

Experimental

Instruments. The ^1H and ^{19}F NMR spectra were recorded by a Bruker Avance500 NMR spectrometer. ^1H and ^{19}F NMR chemical shift were reported relative to residual $CHCl_3$ (7.24 ppm) and $CFCl_3$ (0 ppm), respectively. The UV–vis spectra were recorded using a Shimadzu UV-3150 double beam spectrometer with a thermostated cell holder having a 0.1 °C deviation. The MALDI-TOF-MS was carried out using a mass spectrometer equipped

Published on the web January 10, 2008; doi:10.1246/bcsj.81.76

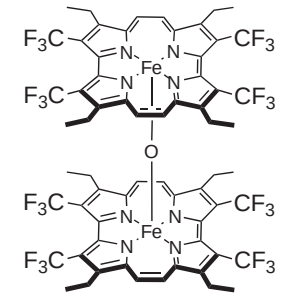

[{$Fe^{III}Etio(CF_3)_4Pc$}$_2$(μ-O)] (**1**)

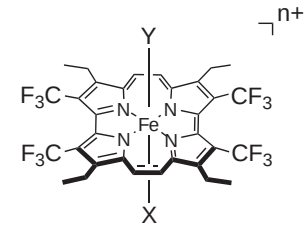

X = Cl, Y = (none), n = 0:
[$Fe^{III}ClEtio(CF_3)_4Pc$] (**2-Cl**)
X = Y = Py, n = 1:
[$Fe^{III}Etio(CF_3)_4Pc(py)_2]^+$ (**2-Py$_2$**)
X = Y= Py, n = 0:
[$Fe^{II}Etio(CF_3)_4Pc(py)_2$] (**7**)

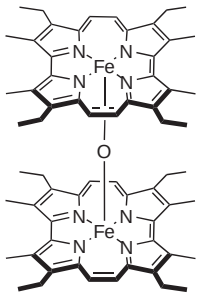

[{$Fe^{III}Etio(CH_3)_4Pc$}$_2$(μ-O)] (**3**)

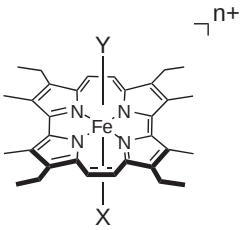

X = Cl, Y = (none), n = 0:
[$Fe^{III}ClEtio(CH_3)_4Pc$] (**4-Cl**)
X = Y = Py, n = 1:
[$Fe^{III}Etio(CH_3)_4Pc(py)_2]^+$ (**4-Py$_2$**)

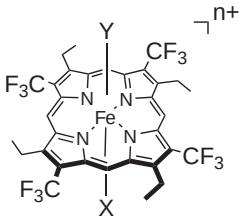

X = Cl, Y = (none), n = 0:
[$Fe^{III}ClEtio(CF_3)_4Por$] (**5-Cl**)
X = Y = Py, n = 1:
[$Fe^{III}Etio(CF_3)_4Por(py)_2]^+$ (**5-Py$_2$**)

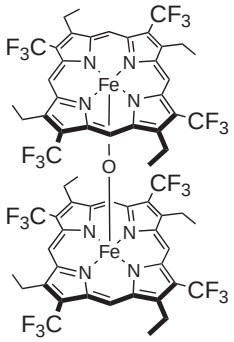

[{$Fe^{III}Etio(CF_3)_4Por$}$_2$(μ-O)] (**6**)

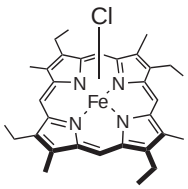

[{$Fe^{III}ClEtio(CH_3)_4Por$] (**8**)

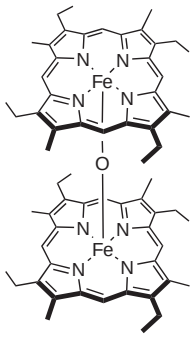

[{$Fe^{III}Etio(CH_3)_4Por$}$_2$(μ-O)] (**9**)

Chart 1.

from an Applied Biosystems Voyager. The electrochemical studies were performed by BAS Bioanalytical System CV-50W electrochemical workstations with a platinum wire as the counter electrode. A Ag/AgCl (saturated NaCl) electrode obtained from BAS, Inc., was used as the reference electrode. The working electrode was a polished disk containing platinum materials.

Chemicals. All reagents and chemicals were obtained from commercial sources and used as received unless otherwise noted. For all the measurements, dichloromethane was distilled over calcium hydride prior to use. Pyridine was carefully distilled over potassium hydroxide prior to use. The kinetic studies were carried out in pyridine and $CHCl_3$ (1:1 v/v). The dehydrated $CHCl_3$ with amylene added was obtained from Wako Pure Chemical Industries, Ltd. Tetrabutylammonium perchlorate (TBAP) was recrystallized from ethanol and then dried under reduced pressure prior to use. Compounds **1** and **2-Cl** were prepared in the same manner as in previous studies.[11] The compounds **3** and **4-Cl** were prepared as described in the literature.[17] Compound **5-Cl** was prepared by a modified method.[19,20]

Synthesis of [$Fe^{III}ClEtio(CF_3)_4Por$] (5-Cl). To a solution of 10 mg of $Etio(CF_3)_4PorH_2$ in 15 mL of acetic acid was dropwise added a mixture of 80 mg of iron(II) sulfate and 80 mg of sodium chloride in 0.2 mL of water and 0.4 mL of pyridine. The mixture was stirred at 130 °C for 40 min. After cooling to room temperature, 50 mL of $CHCl_3$ was added and the solution was washed with 3 M HCl. The organic layer was separated and washed with water twice. The solvent was evaporated and the residue was purified with $CHCl_3$ on TLC. The product was isolated in 44% yield (5 mg). ^{1}H NMR (500 MHz, $CDCl_3$) δ 33.3 (br s, 8H), 6.3 (br s, 12H), −68.5 (br s, 4H); ^{19}F NMR (470 MHz, $CDCl_3$) δ 8.79 (br s); TOF MS (MALDI) m/z calculated for $[M - Cl]^+$ 748.1; found 748.4; UV–vis ($CHCl_3$) λ_{max}, nm (ε, $M^{-1}\,cm^{-1}$) 369 (26500), 409 (76300), 507 (7600), 535 (5300), 634 (1100).

Synthesis of [{$Fe^{III}Etio(CF_3)_4Por$}$_2$(μ-O)] (6). Compound **6**

Table 1. Summary of Structure Determination of [Fe^{II}Etio-$(CF_3)_4$Pc$(py)_2$] (**7**)

Formula	$C_{42}H_{34}F_{12}FeN_6$
Formula weight	906.60
T/K	100(2)
λ/Å	0.71073
Crystal system	Monoclinic
Space group	$C2/m$
Cell constants	
a/Å	14.1005(17)
b/Å	14.8043(18)
c/Å	10.0704(12)
β/deg	114.858(2)
V/Å^3	1907.4(4)
Z	2
D_{calcd}/Mg m^{-3}	1.579
μ (Mo Kα)/mm^{-1}	0.496
Crystal size/mm^3	0.20 × 0.05 × 0.03
θ/deg	2.10–26.37
No. of reflection	6177
No. of independent reflection	2028
No. of parameters	150
Data/parameters	13.52
$R1$[a)]	0.0459
Goodness-of-fit on F^2	1.039
$wR2$[a)]	0.1056

a) Observation criterion $I > 2\sigma(I)$.

was obtained by treating with NaOH (1 M) in CH_2Cl_2 and then purified by chromatography (Silica, CH_2Cl_2) to give a brown solid. The product was isolated in 37% yield. ^{1}H NMR (500 MHz, $CDCl_3$) δ 6.97 (br s, 4H), 6.03 (br s, 4H), 4.88 (br s, 4H), 1.80 and 1.74 (br s, 12H, regioisomer); ^{19}F NMR (470 MHz, $CDCl_3$) δ −47.3 and −47.5 (br s, regioisomer); FAB-MS contains only a signal of the fragment ion produced by the cleavage of Fe–O bond; m/z calculated for $[M - C_{32}H_{24}F_{12}N_4FeO]^+$ 748.1169; found 748.1159; UV–vis ($CHCl_3$) λ_{max}, nm (ε, M^{-1} cm^{-1}) 326 (32900), 404 (103000), 569 (9400).

Crystal Structure Determination. A suitable crystal (0.20 × 0.05 × 0.03 mm^3) of the 2,7,12,17-tetraethyl-3,6,13,16-tetrakis(trifluoromethyl)porphycenatoiron(II) bispyridine complex [Fe^{II}Etio$(CF_3)_4$Pc$(py)_2$] (**7**) was attached to a glass fiber and transferred to a Bruker SMART APEX diffractometer with graphite-monochromated Mo Kα X-radiation (λ = 0.71073 Å), a 2 kW rotating anode generator and a CCD area detector. The data were collected at 100 or 173 K by a cooled nitrogen gas stream with a maximum 2θ value of 54° in 0.30° oscillations with 32 s frame exposures. The data frames were integrated using SAINT (version 6.45) and merged to give a unique data set for the structure determination.[21] SADABS software was used for the absorption corrections.[22] The structure of the complex was solved by direct methods and difference Fourier synthesis using SHELXS-97 and SHELXL-97.[23] Full-matrix least-squares refinements on F^2, using all the data, were carried out with anisotropic displacement parameters applied to all non-hydrogen atoms. The hydrogen atoms were added to the calculated positions and included as riding contributions with isotropic displacement parameters tied to those of the carbon atoms to which they were attached. The crystallographic details for all complexes are presented in Table 1. A selection of important bond distances and angles is depicted in Table 2. Crystallographic data for **7** have been deposited with Cambridge Crystallographic Data Centre, CCDC No. 651038. Copies of the data can be obtained free of charge via http://www.ccdc.cam.ac.uk/conts/retrieving.html (or from the Cambridge Crystallographic Data Centre, 12, Union Road, Cambridge, CB2 1EZ, UK; Fax: +44 1223 336033; e-mail: deposit@ccdc.cam.ac.uk).

Table 2. Selected Bond Distances and Angles for [Fe^{II}Etio-$(CF_3)_4$Pc$(py)_2$] (**7**)

Bond	Distance/Å	Angle[a)]	Angle/deg
Fe–N(1)	1.9582(19)	N(1)–Fe(1)–N(1)#3	180.00(12)
Fe–N(2)	2.007(3)	N(1)#2–Fe(1)–N(1)#3	81.64(11)
N(1)–C(1)	1.377(3)	N(1)–Fe(1)–N(1)#2	98.36(11)
N(1)–C(4)	1.366(3)	N(1)–Fe(1)–N(2)	90.35(8)
		N(1)#3–Fe(1)–N(2)	89.65(8)
		N(1)#1–Fe(1)–N(1)#2	180.0

a) Code of equivalent symmetry positions: #1 $-x$, y, $1 - z$; #2 x, $-y$, z; #3 $-x$, $-y$, $1 - z$.

Kinetic Measurements. All the kinetic measurements were carried out in mixed solvents of $CHCl_3$ and pyridine (1:1, v/v) at 20 °C. Autoreduction of the porphycenes and porphyrins was followed by the ^{19}F NMR and/or UV–vis spectroscopies. The rate constants of the autoreductions for **1**, **2-Cl**, and **6** were determined by analyzing the peak integrations for the iron(III) species and the iron(II) species in the ^{19}F NMR spectra according to first-order kinetics law. Furthermore, the rate constants for **1** and **5-Cl** were measured by UV–vis spectroscopy, where the absorbance changes at 367 nm for **1**, and at 415 nm for **5-Cl** during the reactions, were analyzed by the single-exponential kinetics.

Results and Discussion

Synthesis and Characterization of [{Fe^{III}Etio$(CF_3)_4$Pc}$_2$(μ-O)] (1) and [Fe^{III}ClEtio$(CF_3)_4$Pc] (2-Cl). The preparation of the iron porphycene **1** was reported in our previous paper.[11] The corresponding monomeric complex **2-Cl** was not available because the formation of the μ-oxo dimer was preferable even under the neutral conditions. After the treatment of CF_3COOH/HClaq for over 30 min at room temperature, the monomeric **2-Cl** was obtained, however, further purification of the monomeric complex was difficult, because **2-Cl** was easily converted into the μ-oxo dimer **1** again in the solution. The UV–vis spectra of **1** and **2-Cl** are shown in Fig. 1 together with those of the corresponding reference iron porphycenes, **1** and **2-Cl**. The Q-band absorptions of **1** and **2-Cl** exhibited significant red shifts compared to those of **3** and **4-Cl** in CH_2Cl_2. For example, the characteristic Q-band of **2-Cl** is located at 687 nm, which is 69 nm red-shifted from that of **4-Cl**. These significant red shifts are similar in behavior to a series of perhaloganoporphyrin iron complexes,[24] indicating that the four trifluoromethyl groups at the pyrrolic β-carbons effectively regulate the electronic properties of the iron porphycene complexes.

Redox Potentials of Trifluoromethylated Iron Porphycene. The Fe^{II}/Fe^{III} redox couple of **2-Cl** displayed in Fig. 2 is observed at the potential of −0.02 V (vs. Ag/AgCl) in CH_2Cl_2. As shown in Table 3, this potential is anodically shifted by more than 250 mV from that of **4-Cl** due to the introduction of the four electron-withdrawing trifluoromethyl groups, whereas the corresponding trifluoromethylated iron

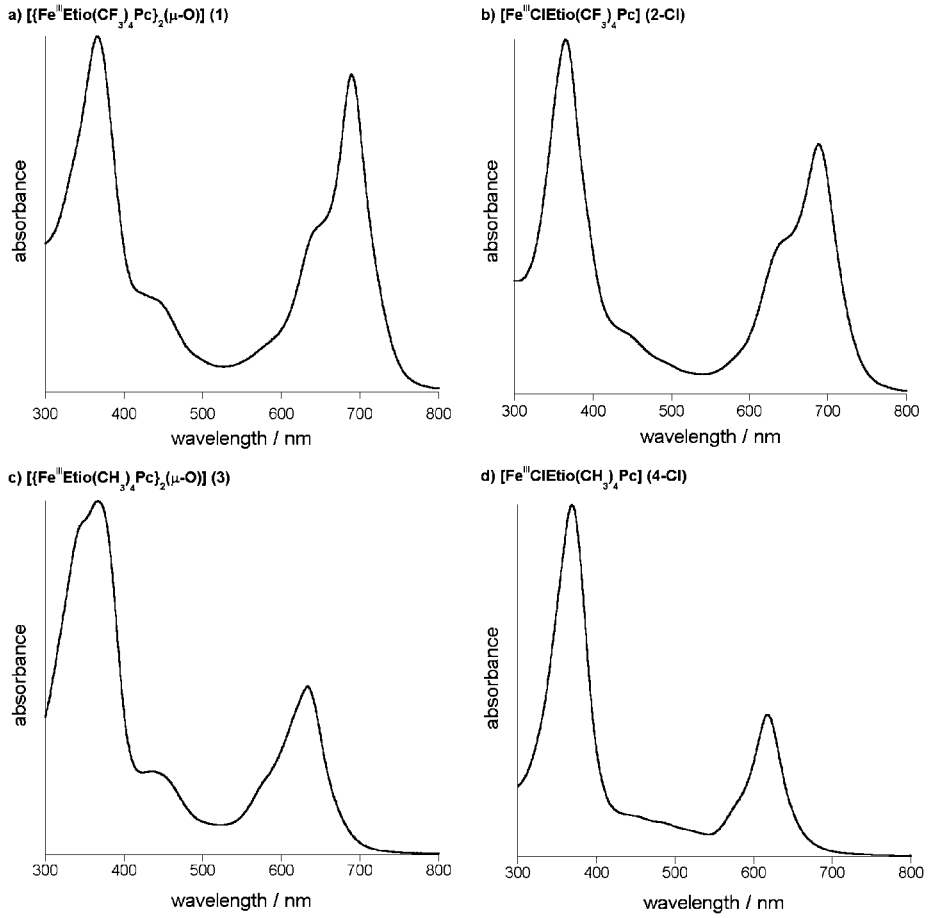

Fig. 1. UV–vis spectra of (a) [{Fe^{III}Etio$(CF_3)_4$Pc}$_2(\mu$-O)] (**1**), (b) [Fe^{III}ClEtio$(CF_3)_4$Pc] (**2-Cl**), (c) [{Fe^{III}Etio$(CH_3)_4$Pc}$_2(\mu$-O)] (**3**), and (d) [Fe^{III}ClEtio$(CH_3)_4$Pc] (**4-Cl**) in CH_2Cl_2. Each absorption maximum is normalized by setting the highest absorbance (Soret band) equal to unity.

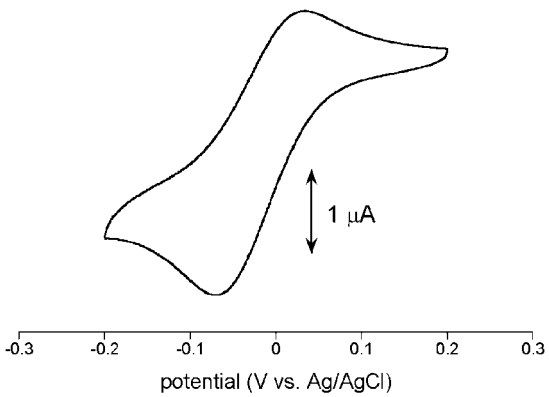

Fig. 2. Cyclic voltammogram for the Fe^{II}/Fe^{III} reaction of [Fe^{III}ClEtio$(CF_3)_4$Pc] (**2-Cl**) in CH_2Cl_2, 0.1 M TBAP.

porphyrin, **5-Cl**, exhibited the same potential. It is not surprising that the redox potential of **2-Cl** is comparable to that of **5-Cl**.[25] This is the same behavior for the Fe^{II}/Fe^{III} redox couple that is moderately different between **4-Cl** and [Fe^{III}ClEtio$(CH_3)_4$Por] (**8**). Therefore, the symmetry of the macrocycle does not have any significant influence on the redox potential. In any event, the introduction of four trifluoromethyl groups into the β-pyrrolic carbons of the porphycene ring may stabilize the iron(II) oxidation state.

Table 3. Half-Wave Potentials (V vs. Ag/AgCl) for Metal Reduction and Oxidation of Iron Complexes in CH_2Cl_2, 0.1 M TABP at 25 °C[a)]

Iron complexes	$E_{1/2}$ (V vs. Ag/AgCl) Fe^{II}/Fe^{III}
2-Cl	−0.02
4-Cl	$(-0.48)E_{pc}$, $(-0.09)E_{pa}$
5-Cl	0.00
8	−0.57

a) Scan rate = 0.1 V s^{-1}.

Autoreduction of μ-Oxo Dimer of Iron Porphycenes and Porphyrins in Pyridine. In our previous study, it was found that the iron μ-oxo dimer **1** was converted into the monomeric iron(II) species via the Fe–O bond cleavage in pyridine under the aerobic conditions.[11] The UV–vis spectroscopic studies demonstrated the conversion from the iron(III) **1** to the iron(II) form without any intermediate, such as the monomeric iron(III) complex. Furthermore, we have recently monitored the autoreduction of **1** by ^{19}F NMR spectroscopy, showing that the signal of **1** at −44.70 ppm assigned to the $C^{19}F_3$ groups disappeared after 1 day along with the increasing intensity at −53.21 ppm due to the iron(II) species. In contrast, no monomeric [Fe^{III}Etio$(CF_3)_4$Pc$(py)_2]^+$ (**2-Py$_2$**) was detected during

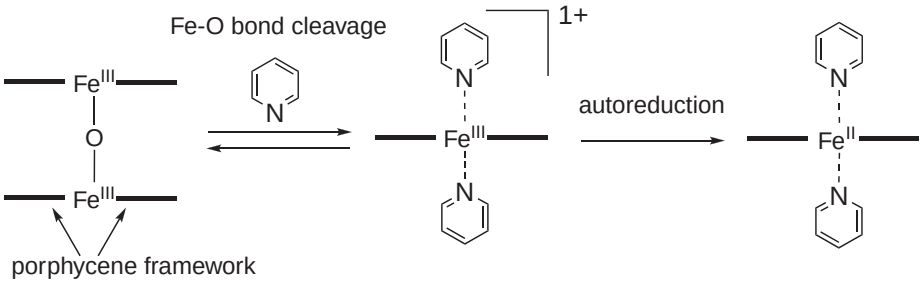

Scheme 1.

the conversion of **1** to the iron(II) species.[26] The autoreduction product, the iron(II) complex, was also characterized by UV–vis and ^{1}H NMR spectroscopies and an X-ray structural analysis (vide infra). Based on these findings, we concluded that the autoreduction of **1** smoothly proceeded after the Fe–O bond cleavage of the μ-oxo dimer as shown in Scheme 1.

Crystal Structure of the Reaction Product. Figure 3 presents the molecular structure of the autoreduction product recrystallized from chloroform including pyridine (1:1, v/v). The iron porphycene in the monoclinic system with the space group $C2/m$ has both a crystallographically required 2-fold axis and a mirror plane of symmetry, with the iron atom at a symmetry center. Two pyridine molecules coordinated to the iron atom were found in the complex with an eclipsed conformation. The porphycene framework is slightly distorted, whereas the iron atom is located inside the plane; the displacements of the C_β carbon atoms from the least-squares plane defined by the four central nitrogen atoms are determined to be $\pm$0.224 and $\pm$0.313 Å, and those of C_α and $C_{ethylene}$ are $\pm$0.085 and $\pm$0.045 Å, respectively.

Table 4 displays an informative comparison with the series of low-spin bispyridine iron(II) complexes. The magnitudes of the perpendicular displacements of these carbon atoms from the plane of the four pyrrolyl nitrogen atoms for [Fe^{II}-Etio(CF$_3$)$_4$Pc(py)$_2$] (**7**) are clearly smaller than those of the iron porphyrin bispyridine complexes with electron-withdrawing substitutes.[18,27,28] However, as seen in Table 4, the Fe–N$_{pyridyl}$ (2.007 Å) and Fe–N$_{pyrrolyl}$ (1.958 Å) bonds in **7** reveal remarkably short distances among the bispyridine-coordinated iron(II) porphyrins.[28–30] Particularly, the short Fe–N$_{pyridyl}$ bond lengths in **7** suggest that the electron-deficient iron atom in the porphycene ring having the four strong electron-withdrawing CF$_3$ groups tightly interacts with the pyridine molecule with a strong Lewis basicity. Moreover, the

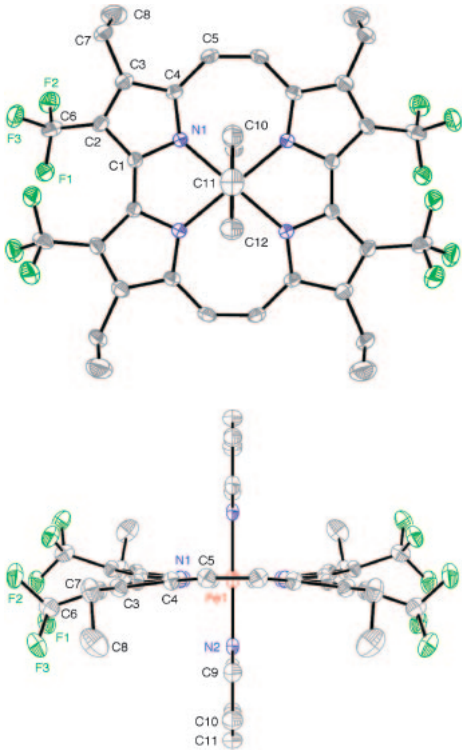

Fig. 3. ORTEP diagrams of [Fe^{II}Etio(CF$_3$)$_4$Pc(py)$_2$] (**7**) with ellipsoids drawn at the 50% probability level.

relative orientation of the two axial pyridine planes of **7** is quite different from those of the other low-spin iron(II) complexes having electron-withdrawing groups,[27,28] whereas it is known that the bispyridine iron(II) complex of the tetraphenylporphyrin [Fe^{II}(C$_6$H$_5$)$_4$Por(py)$_2$] without any electron-withdrawing groups exhibit a similar eclipsed configuration of

Table 4. Selected Bond Distances and Angles for Bispyridine-Coordinated Iron(II) Complexes

Iron complexes	Fe–N$_{pyridyl}$ distance/Å	Fe–N$_{pyrrole}$ distance/Å	bis(py)$_2$ relative orientation/°[d]	C$_{(methylene\ or\ meso)}$ deviation/Å[e]	C$_\beta$ deviation/Å[f]	Reference
7	2.007	1.958	0.0	0.05	0.27	this work
[Fe^{II}(C$_3$F$_7$)$_4$Por(py)$_2$][a]	2.002	1.958	87.5	0.62	0.24	27
[Fe^{II}(C$_6$F$_5$)$_4$Br$_8$Por(py)$_2$][b]	2.012	1.963	68.3	0.11	0.97	28
[Fe^{II}(C$_6$H$_5$)$_4$Por(py)$_2$][c]	2.037	2.001	4.8	0.10	0.25	29

a) [Fe^{II}(C$_3$F$_7$)$_4$Por(py)$_2$] = bispyridine-5,10,15,20-tetrakis(heptafluoropropyl)porphyrinatoiron(II). b) [Fe^{II}(C$_6$F$_5$)$_4$Br$_8$-Por(py)$_2$] = bispyridine-2,3,7,8,12,13,17,18-octabromo-5,10,15,20-tetrakis(pentafluorophenyl)porphyrinatoiron(II). c) [Fe^{II}(C$_6$H$_5$)$_4$Por(py)$_2$] = bispyridine-5,10,15,20-tetraphenylporphyrinatoiron(II). d) Defined as the torsional angle between two planar pyridines. e) Defined as the average value of methylene or *meso*-carbon atom deviation from the N4 mean plane. f) Defined as the average value of β-carbon atom deviation from the N4 mean plane.

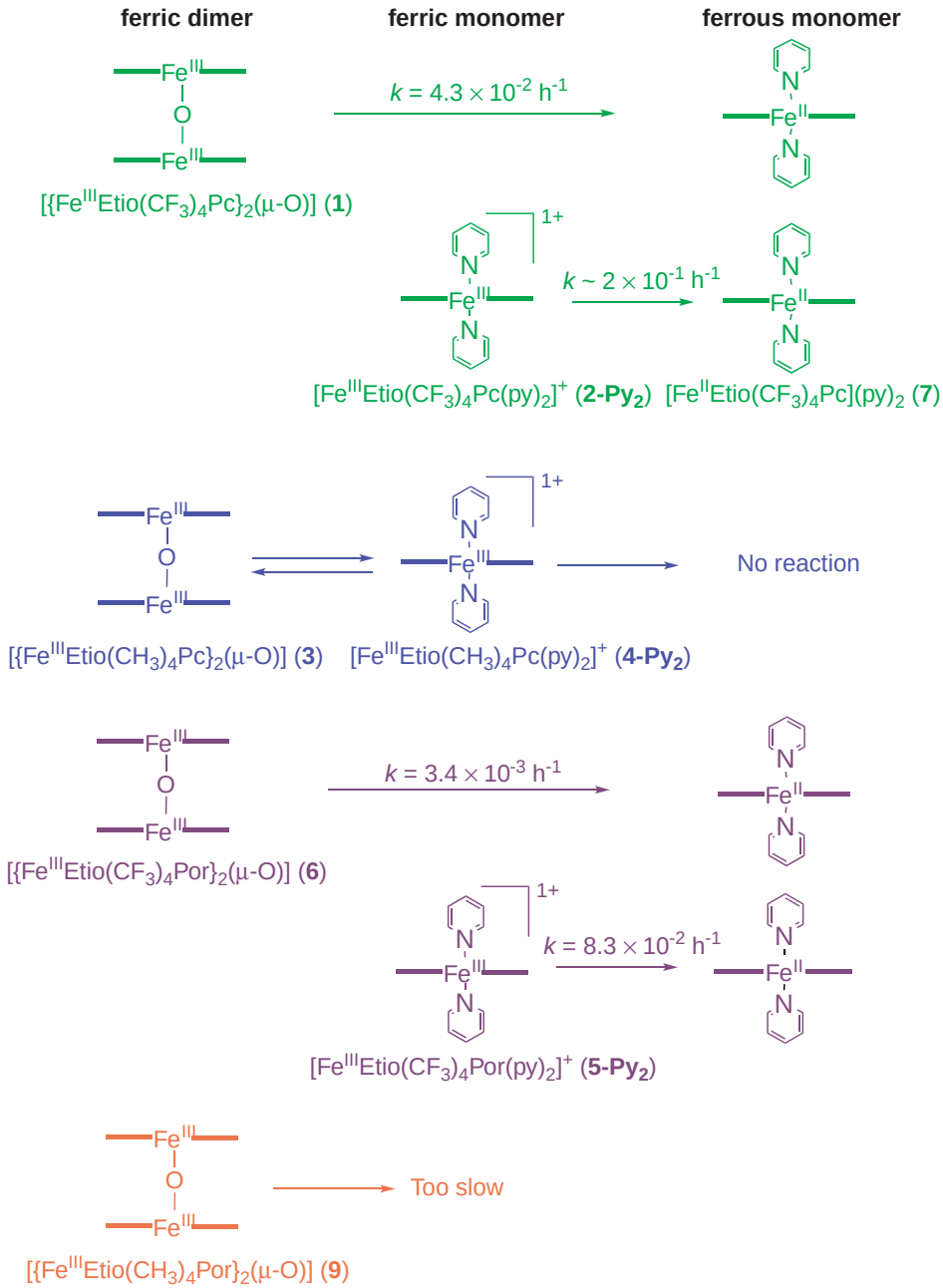

Scheme 2.

two pyridine planes as **7**.[29] It is likely that the four trifluoromethyl substituents in **7** produce no serious strain on the porphycene framework, and the two axial ligands are consequently eclipsed in the complex, which features a relatively planar porphyrin macrocycle.[29]

In addition, surprisingly, the crystal of the bispyridine–iron(II) porphycene complex was not oxidized even under aerobic conditions for over a month, suggesting that the bispyridine complex of the iron(II) porphycene is extremely stable.

Kinetic Study of the Autoreduction from Iron(III) μ-Oxo Dimer Complexes. To evaluate the influence of the CF_3 substituents and framework structure on the autoreduction from the iron(III) μ-oxo dimers via the Fe–O bond cleavage, we compared the reactivities of **1** in pyridine with the reference iron porphycene and porphyrins. Scheme 2 summarizes the rates of the sequential two-step reactions of the iron porphycene and porphyrin compounds. The rate constants depicted in Scheme 2 were determined by the ^{1}H or ^{19}F NMR and/or UV–vis spectroscopic analyses shown in Fig. 4. First of all, it is clear that the Fe–O bond cleavages of the μ-oxo dimers of the iron porphycenes occurred at the initial stage of the reactions are faster than those of the iron porphyrins, regardless of whether or not there are electron-withdrawing groups at the peripheral positions of the porphycene framework. It is known that the equilibrium between the two iron species is shifted to the μ-oxo dimer in the iron porphyrin chemistry. Therefore, the unusual equilibrium shifted to the monomeric species,

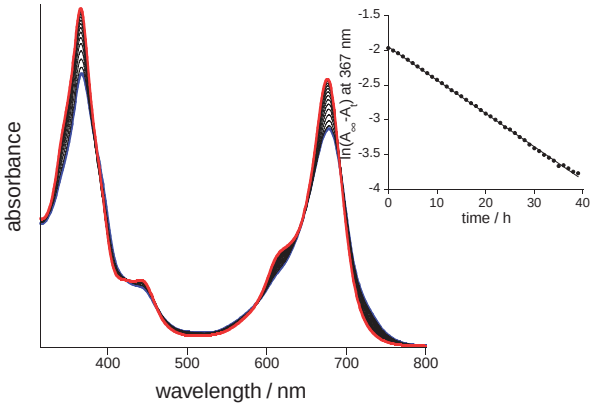

Fig. 4. UV–vis spectral changes in the autoreduction from [{Fe^{III}Etio$(CF_3)_4$Pc}$_2$(μ-O)] (**1**) (blue line) to [Fe^{II}Etio$(CF_3)_4$Pc(py)$_2$] (**7**) (red line) in $CHCl_3$/pyridine (1:1, v/v) at 20 °C for 45 h. The inset is a plot of $\ln(A_\infty - A_t)$ at 367 nm vs. time, where A_∞ and A_t stand for the absorbances at the completion of the reaction and at certain time, respectively.

i.e., from **1** and **3** to **2-Py$_2$** and [Fe^{III}Etio$(CH_3)_4$Pc(py)$_2$]$^+$ (**4-Py$_2$**) respectively, in pyridine supports the facts that the pyridine-ligated monomeric iron porphycenes are thermodynamically more stable than the corresponding μ-oxo dimers. This finding can be explained by the increase in the Lewis acidity of the central iron atom in the porphycene frameworks;[31,32] the strong binding of pyridine promotes the Fe–O bond cleavage. In addition, it is known that the Fe–O bond cleavage of the μ-oxo dimer in pyridine is also observed for the iron dioxoporphodimethene complex.[35]

Second, the autoreduction reactivities between **1** and **3** are quite different. As described above, the Fe–O bond cleavage and the following autoreduction of **1** smoothly proceeded with the overall rate constant of 4.3×10^{-2} h^{-1} in $CHCl_3$/pyridine (1:1, v/v) at 20 °C, whereas the reaction of **3** stopped at the formation of the monomeric iron(III) porphycene, and the diamagnetic iron(II) complex was not detected in $CDCl_3$/pyridine-d_5 (1:1, v/v) by ^{1}H NMR spectroscopy. The monomeric iron porphycene with CF_3 groups, **2-Cl**, was also converted into the iron(II) complex with the rate constant of $\approx 2 \times 10^{-1}$ h^{-1},[34] while **4-Cl** as the starting material was not reduced in $CHCl_3$/pyridine (1:1, v/v). On the other hand, both **5-Cl** and **6** allowed the autoreduction upon dissolution in $CHCl_3$/pyridine (1:1, v/v) at room temperature. The reaction from the monomeric species, **5-Cl** is much slower by 2-fold than that observed for **2-Cl**, and the overall reaction from the corresponding μ-oxo dimer, **6**, took over one month.[35] Moreover, neither [Fe^{III}ClEtio$(CH_3)_4$Por] (**8**) nor its μ-oxo dimer (**9**) showed any reactions in $CHCl_3$/pyridine (1:1, v/v). These findings suggest that the autoreduction of the tetrapyrrole iron complexes mainly depend on the Fe^{II}/Fe^{III} redox potential in spite of the structure of the macrocyclic ligands, i.e., more positive the redox potential, more readily the autoreduction proceeds.

Summary

It is well-known that most iron(II) complexes with a series of tetrapyrrolic ligands autoxidize to the corresponding iron(III) species and/or μ-oxo dimers. However, in the present study, we successfully obtained the clearly stable iron(II) porphycene complex linked by four strong electron-withdrawing groups, CF_3 substituents, upon dissolution of the corresponding iron(III) μ-oxo dimer in pyridine. The Fe–O bond cleavage and the following autoreduction was also reported by iron dioxoporphodimethene complex for over one week at room temperature,[33] whereas the present μ-oxo dimer of the iron porphycene is more readily cleaved and reduced in pyridine after one day at room temperature. Moreover, to the best of our knowledge, the crystal structure of [Fe^{II}Etio$(CF_3)_4$Pc(py)$_2$] (**7**) is the first example of a 6-coordinate low-spin iron(II) porphycene complex, although there is only one report describing the 4-coordinated iron(II)porphycene without any axial ligands.[36] The Fe–$N_{pyridyl}$ and Fe–$N_{pyrrolyl}$ bond lengths of our iron(II) complex are remarkably shortened as seen in the special iron porphyrin with C_3F_7 groups at each *meso*-position,[27] whereas the structure of the macrocycle and the two axial ligand configurations are relatively similar to those of [Fe^{II}-$(C_6H_5)_4$Por(py)$_2$]. It is concluded that the attractive physicochemical property of the present iron porphycene with four CF_3 groups is due to the strong Lewis acidic iron atom and highly positive Fe^{II}/Fe^{III} redox potential.

This work was partially supported by the Ministry of Education, Culture, Sports, Science and Technology. K.I. received the financial support from the Japan Society for the Promotion of Science (JSPS) Research Fellowships for Young Scientists. T.M. is grateful for Mitsubishi Chemical Corporation Fund. We thank Dr. Nobuko Kanehisa (Osaka University) for her kind help with X-ray analyses.

Supporting Information

Crystal structure data of [Fe^{II}Etio$(CF_3)_4$Pc(py)$_2$] (**7**) are available in Tables S1–S4 in Supporting Information. This material is available free of charge on the web at http://www.csj.jp/journals/bcsj/.

References

This paper is dedicated to the memory of late Professor Yoshihiko Ito, Emeritus Professor of Kyoto University.

1 E. Vogel, M. Köcher, H. Schmickler, J. Lex, *Angew. Chem., Int. Ed. Engl.* **1986**, *25*, 257.

2 C. Bernard, J. P. Gisselbrecht, M. Gross, E. Vogel, M. Lausmann, *Inorg. Chem.* **1994**, *33*, 2393.

3 M. W. Renner, A. Forman, W. Wu, C. K. Chang, J. Fajer, *J. Am. Chem. Soc.* **1989**, *111*, 8618.

4 J. P. Gisselbrecht, M. Gross, M. Köcher, M. Lausmann, E. Vogel, *J. Am. Chem. Soc.* **1990**, *112*, 8618.

5 F. D'Souza, M. E. Zandler, P. Tagliatesta, Z. Ou, J. Shao, E. V. Caemelbecke, K. M. Kadish, *Inorg. Chem.* **1998**, *37*, 4567.

6 J. A. Hodge, M. G. Hill, H. B. Gray, *Inorg. Chem.* **1995**, *34*, 809.

7 J. G. Goll, K. T. Moore, A. Ghosh, M. J. Therien, *J. Am. Chem. Soc.* **1996**, *118*, 8344.

8 Y. Terazono, B. O. Patrick, D. H. Dolphin, *Inorg. Chem.* **2002**, *41*, 6703.

9 Y. Terazono, D. H. Dolphin, *J. Org. Chem.* **2003**, *68*, 1892.

10 T. Hayashi, Y. Nakashima, K. Ito, T. Ikegami, I. Aritome, A. Suzuki, Y. Hisaeda, *Org. Lett.* **2003**, *5*, 2845.

11 T. Hayashi, Y. Nakashima, K. Ito, T. Ikegami, I. Aritome, K. Aoyagi, T. Ando, Y. Hisaeda, *Inorg. Chem.* **2003**, *42*, 7345.

12 S. Will, A. Rahbar, H. Schmichkler, J. Lex, E. Vogel, *Angew. Chem., Int. Ed. Engl.* **1990**, *29*, 1390.

13 W. A. Oertling, W. Wu, J. López-Garriga, Y. Kim, C. K. Chang, *J. Am. Chem. Soc.* **1991**, *113*, 127.

14 T. Baba, H. Shimakoshi, I. Aritome, Y. Hisaeda, *Chem. Lett.* **2004**, *33*, 906.

15 E. Vogel, M. Köcher, J. Lex, E. Johann, O. Ermer, *Isr. J. Chem.* **1989**, *29*, 257.

16 J. L. Sessler, A. Gebauer, E. Vogel, in *The Porphyrin Handbook*, ed. by K. M. Kadish, K. M. Smith, R. Guilard, Academic Press, San Diego, **2000**, Vol. 2, pp. 3–14.

17 J. L. Sessler, S. J. Weghorn, *Expanded, Contracted & Isomeric Porphyrins*, Elsevier, New York, **1997**, Vol. 15, pp. 127–147.

18 [{Fe^{III}Etio$(CF_3)_4$Pc}$_2(\mu$-O)] (**1**) = μ-Oxo-bis{2,7,12,17-tetraethyl-3,6,13,16-tetrakis(trifluoromethyl)porphycenatoiron(III)}. [Fe^{III}ClEtio$(CF_3)_4$Pc] (**2-Cl**)=Chloro-2,7,12,17-tetraethyl-3,6,13,16-tetrakis(trifluoromethyl)porphycenatoiron(III). [Fe^{III}Etio$(CF_3)_4$Pc(py)$_2$]$^+$ (**2-Py$_2$**) = Bispyridine-2,7,12,17-tetraethyl-3,6,13,16-tetrakis(trifluoromethyl)porphycenatoiron(III). [{Fe^{III}Etio$(CH_3)_4$Pc}$_2(\mu$-O)] (**3**) = μ-Oxo-bis{2,7,12,17-tetraethyl-3,6,13,16-tetramethylporphycenatoiron(III)}. [Fe^{III}ClEtio$(CH_3)_4$Pc] (**4-Cl**) = Chloro-2,7,12,17-tetraethyl-3,6,13,16-tetramethylporphycenatoiron(III). [Fe^{III}Etio$(CH_3)_4$Pc(py)$_2$]$^+$ (**4-Py$_2$**) = Bispyridine-2,7,12,17-tetraethyl-3,6,13,16-tetramethylporphycenatoiron(III). [Fe^{III}ClEtio$(CF_3)_4$Por] (**5-Cl**) = Chloro-1,3,5,7-tetrakis(trifluoromethyl)-2,4,6,8-tetraethylporphyrinatoiron(III). [Fe^{III}Etio$(CF_3)_4$Por(py)$_2$]$^+$ (**5-Py$_2$**) = Bispyridine-1,3,5,7-tetrakis(trifluoromethyl)-2,4,6,8-tetraethylporphyrinatoiron(III). [{Fe^{III}Etio$(CF_3)_4$Por}$_2(\mu$-O)] (**6**) = μ-Oxo-bis{1,3,5,7-tetrakis(trifluoromethyl)-2,4,6,8-tetraethylporphyrinatoiron(III)}. [Fe^{II}Etio$(CF_3)_4$Pc(py)$_2$] (**7**) = Bispyridine-2,7,12,17-tetraethyl-3,6,13,16-tetrakis(trifluoromethyl)-porphycenatoiron(II). [Fe^{III}ClEtio$(CH_3)_4$Por] (**8**) = Chloro-1,3,5,7-tetraethyl-2,4,6,8-tetramethylporphyrinatoiron(III). [{Fe^{III}Etio$(CH_3)_4$Por}$_2(\mu$-O)] (**9**) = μ-Oxo-bis{1,3,5,7-tetramethyl-2,4,6,8-tetraethylporphyrinatoiron(III)}.

19 N. Ono, H. Kawamura, K. Maruyama, *Bull. Chem. Soc. Jpn.* **1989**, *62*, 3386.

20 T. Yoshimura, H. Toi, S. Inaba, H. Ogoshi, *Inorg. Chem.* **1991**, *30*, 4315.

21 *SAINT Software Package, Version 6.45*, Bruker AXS, Inc., Madison, WI 53711-5373, USA, **2001**.

22 G. Sheldrick, *SADABS Software*, University of Göttingen, **1996**.

23 *SHELXS-97 and SHELXL-97 Software Packages*, Bruker AXS, Inc., Madison, WI 5371-5373, USA, **1997**.

24 M. O. Senge, in *The Porphyrin Handbook*, ed. by K. M. Kadish, K. M. Smith, R. Guilard, Academic Press, San Diego, **2000**, Vol. 1, p. 333.

25 F. D'Souza, P. Boulas, A. M. Aukauloo, R. Guilard, M. Kisters, E. Vogel, K. M. Kadish, *J. Phys. Chem.* **1994**, *98*, 11885.

26 ^{19}F NMR chemical shift of **2** was appeared at 67.42 ppm in $CDCl_3$.

27 K. T. Moore, J. T. Fletcher, M. J. Therien, *J. Am. Chem. Soc.* **1999**, *121*, 5196.

28 M. W. Grinstaff, M. G. Hill, E. R. Birnbaum, W. P. Schaefer, J. A. Labinger, H. B. Gray, *Inorg. Chem.* **1995**, *34*, 4896.

29 N. Li, P. Coppens, J. Landrum, *Inorg. Chem.* **1988**, *27*, 482.

30 Although the refinement of the crystal structure of **7** has never been completed, the Fe–$N_{pyridyl}$ and Fe–$N_{pyrrole}$ bond distances were preliminary determined as 2.02 and 2.00 Å, respectively.

31 Pyridine association constants for the monomeric iron complexes (K_1): **2-Cl**, 23 M^{-1}; **4-Cl**, 76 M^{-1}; **5-Cl**, 1.4 M^{-1}; and **8**, 0.41 M^{-1}. The association constants were determined by UV–vis titrimetric measurements in CH_2Cl_2 at 25 °C.

32 C. Bernard, Y. L. Mest, J. P. Gisselbrecht, *Inorg. Chem.* **1998**, *37*, 181.

33 A. L. Balch, B. C. Noll, M. M. Olmstead, S. L. Phillips, *Inorg. Chem.* **1996**, *35*, 6495.

34 It was confirmed that the reaction was completed after 28 h.

35 Labinger, Gray and their co-workers prepared iron(II) porphyrin with multiple electron-withdrawing groups upon dissolution in pyridine for 1 h, although they did not comment on the details.[28]

36 K. Rachlewicz, L. Latos-Grażyński, E. Vogel, Z. Ciunik, L. B. Jerzykiewicz, *Inorg. Chem.* **2002**, *41*, 1979.